



## Systematic studies of timing characteristics for 2 m long scintillation counters

S. Denisov<sup>a,\*</sup>, A. Dzierba<sup>b</sup>, R. Heinz<sup>b</sup>, A. Klimenko<sup>a</sup>, V. Samoylenko<sup>a</sup>,  
E. Scott<sup>b</sup>, P. Smith<sup>b</sup>, S. Teige<sup>b</sup>

<sup>a</sup>*Institute for High Energy Physics, Protvino 142281, Moscow Region, Russian Federation*

<sup>b</sup>*Department of Physics, Indiana University, Bloomington, IN 47405, USA*

---

### Abstract

Timing properties of two types of scintillation counters have been studied in 5 GeV/c hadron beam of the IHEP (Protvino) accelerator. The counters are prototypes of hodoscope elements that will be used in experiments for particle identification and fast timing of events. Scintillator cross-sections are  $1.25 \times 6.0$  and  $2.5 \times 2.5$  cm<sup>2</sup> and their length is 2 m. The dependence of the time resolution on the particle coordinate along the counters and on the beam intensity is presented.

© 2004 Elsevier B.V. All rights reserved.

PACS: 29.40.Mc

Keywords: GlueX; Time of flight; Particle identification

---

### 1. Introduction

The counters investigated are prototypes for the  $2 \times 2$  m<sup>2</sup> X–Y hodoscopes that will be used for particle identification employing the time-of-flight (TOF) technique in the GlueX experiment [1] at Jefferson Lab (Newport News, USA) and for precise timing in the rare charged kaon decay experiment at the Institute for High Energy Physics (Protvino, Russia).

The goal of the TOF system in the GlueX experiment is to discriminate kaons from pions in the momentum range up to 3 GeV/c. The hodoscope time resolution should be less than 80 ps to meet this requirement [1].

The kaon decay experiment will be performed with a high intensity (up to  $\approx 10^8$  particles/s) hadron beam, 10% of which will be kaons. To select detected particles belonging to the same decay by timing, a scintillator hodoscope with a time resolutions of 200 ps will be constructed.

Results of studies of the GlueX hodoscope elements based on 2.5, 5.0 and 6.0 cm thick scintillators were published [2,3]. Since the hodoscope will be installed in front of the electromagnetic lead glass calorimeter, it is important to minimize the amount of material in it. Below we present the timing characteristics of 1.25 cm thick scintillation bars.

Simulations performed indicate that the optimal width of the hodoscope elements for the kaon decay experiment is 2.5 cm. The results of the time resolution measurements for a scintillation bar

---

\*Corresponding author. Fax: +7-0967-745738.

E-mail address: [denisov@mx.ihep.su](mailto:denisov@mx.ihep.su) (S. Denisov).

with  $2.5 \times 2.5 \text{ cm}^2$  cross-section are also presented in our report.

## 2. Experimental setup

Timing measurements were carried out using a  $5 \text{ GeV}/c$  positive hadron beam at the IHEP accelerator. The coincidence of signals from 3 beam counters was used to form a trigger and to define the beam size ( $2.0 \times 2.0 \text{ cm}^2$ ) at the scintillation bars under investigation [2,3]. Timing properties of two bars with a cross-section of  $1.25 \times 6.0 \text{ cm}^2$  and one bar with a  $2.5 \text{ cm}$  square cross-section were studied. The  $2.5 \text{ cm}$  square bar made of scintillator with  $2 \text{ ns}$  decay time and  $4 \text{ m}$  bulk attenuation length produced by the Eljen Corporation [4]. The  $1.25 \times 6.0 \text{ cm}^2$  bars were manufactured of Bicron-404 scintillator with the similar characteristics [5]. All bars were viewed from both ends by Philips XP2020 PMTs. Measurements with a  $2.5 \text{ cm}$  square bar were also performed using a Russian PMT FEU-115M [6] with the  $25 \text{ mm}$  photocathode. The PMTs had an optical contact with the scintillators.

Signals from the PMTs went to constant fraction discriminators (CFDs) via  $40 \text{ m}$  long cables. CFDs allow one to correct for the dependence of timing on signal pulse height. Custom-made 12-bit TDCs with a  $25 \text{ ps}$  least count were used to measure time intervals between the bar signals (STOP signals) and the common START signal from one of the beam counters. The measured time resolution of the trigger counter and intrinsic time resolution of electronics were  $70$  and  $18 \text{ ps}$ , respectively [3].

A typical time spectrum of PMT signals is shown in Fig. 1. All time spectra are well described by a Gaussian. The variance and the average of the Gaussian were used to obtain the time resolution,  $\sigma$ , and the peak position,  $T$ , of the distribution.

## 3. Results

Fig. 2 shows the dependencies of  $T$  on the beam position  $x$  along the bars viewed by the XP2020 PMTs. The slopes of the lines in this diagram

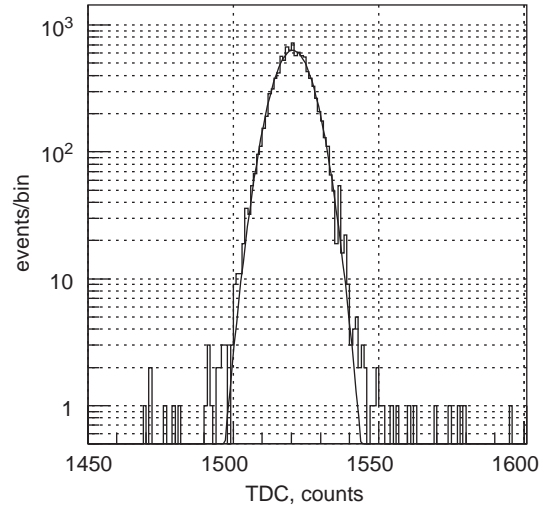


Fig. 1. Time distribution of XP2020 signals at the center of  $1.25 \times 6.0 \text{ cm}^2$  bar.

correspond to the effective speed of light in the  $x$ -direction of  $16.1 \text{ cm/ns}$  for the  $1.25 \text{ cm}$  bar and  $15.7 \text{ cm/ns}$  for the  $2.5 \text{ cm}$  bar. Using the index of refraction  $n = 1.58$ , the average angle of the light with respect to the  $x$ -axis is  $32^\circ$  ( $1.25 \text{ cm}$  bar) and  $34.2^\circ$  ( $2.5 \text{ cm}$  bar). The  $x$ -dependence of  $T$  for FEU-115M has the same slope as for XP2020.

The  $x$ -dependence of the time resolution  $\sigma$  for a single PMT is shown in Figs. 3 and 4. The contribution of the START counter was subtracted quadratically but no corrections were made for the finite size ( $2 \times 2 \text{ cm}^2$ ) of the START counter and the intrinsic time resolution of electronics. The time resolution for one ( $\sigma_1$ ) and two ( $\sigma_2$ ) bars shown in Figs. 5 and 6 was estimated using

$$\frac{1}{\sigma_k^2} = \sum_{i=1}^n \frac{1}{\sigma_i^2} \quad (1)$$

where  $\sigma_i$  is the time resolution of the  $i$ th PMT at given  $x$  and  $n = 2(4)$  for  $k = 1(2)$ . Assuming that

$$\sigma \sim 1/\sqrt{N_p} \text{ and } N_p \sim \exp(-x/\lambda) \quad (2)$$

where  $N_p$  is a number of photoelectrons and  $\lambda$  is the light attenuation length in  $x$ -direction the

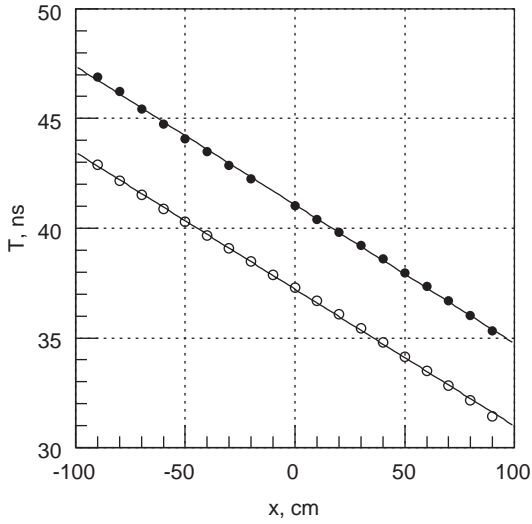


Fig. 2.  $T(x)$  for  $1.25 \times 6.0 \text{ cm}^2$  (○) and 2.5 cm square (●) bars viewed by XP2020 PMTs.

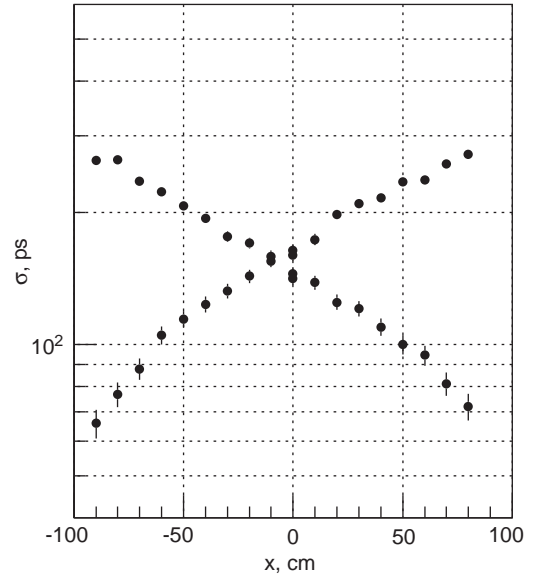


Fig. 4. The time resolution for the  $1.25 \times 6.0 \text{ cm}^2$  bar viewed by XP2020 PMTs.

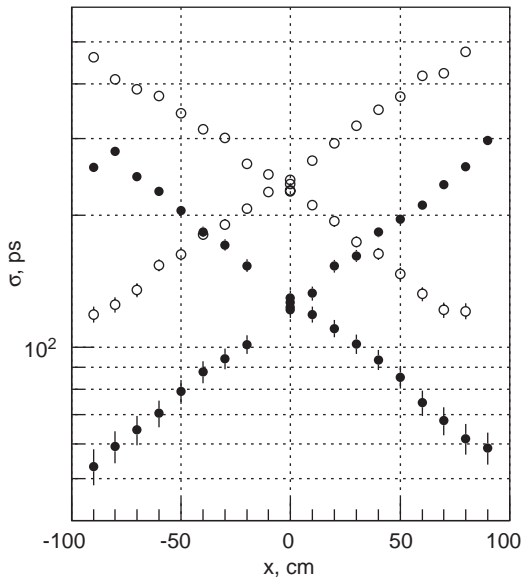


Fig. 3. The  $x$ -dependence of the time resolution of XP2020 (●) and FEU-115M (○) PMTs for the 2.5 cm square bar.

following relation can be derived for  $\sigma_1$  and  $\sigma_2$ :

$$\frac{1}{\sigma_k^2} = \sum_{i=1}^n \frac{1}{\sigma_{0i}^2} \exp\left(\frac{(-1)^i x}{\lambda_k}\right) \quad (3)$$

where  $\sigma_{0i}$  is the time resolution for the  $i$ th channel at  $x = 0$  and  $n = 2(4)$  for  $k = 1(2)$ . The values of

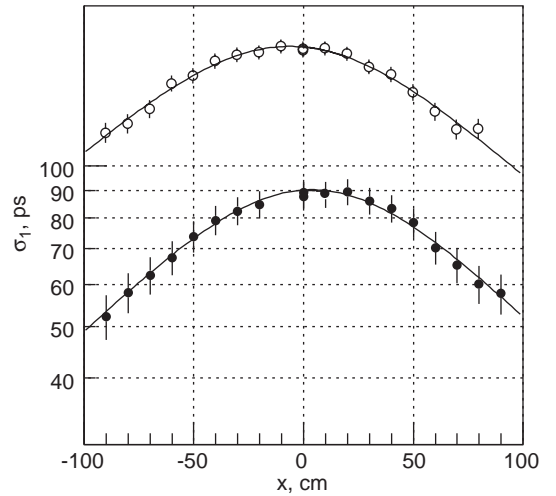


Fig. 5. The time resolution of the 2.5 cm square bar viewed by XP2020 (●) and FEU115 (○) PMTs.

$\sigma_{0i}$  and  $\lambda$  parameters were obtained by fitting experimental data for the individual bars and listed in Table 1. Dependence (3) with the parameters from Table 1 is shown in Figs. 5 and

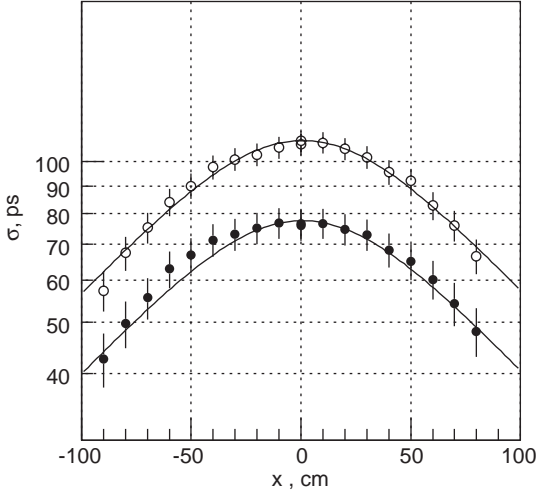


Fig. 6. The time resolution for one (○) and two (●)  $1.25 \times 6.0$  cm<sup>2</sup> bars viewed by XP2020 PMTs.

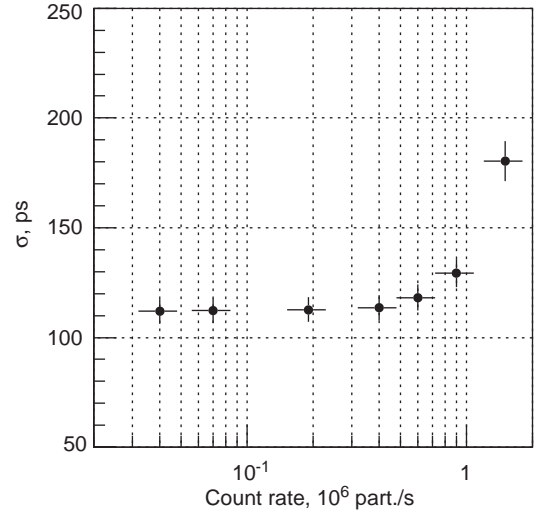


Fig. 7. Time resolution vs counting rate for  $1.25 \times 6.0$  cm<sup>2</sup> bar viewed by XP2020.

Table 1

Bar(s), cross-section (cm <sup>2</sup> )	PMT	$\sigma_{01}$ (ps)	$\sigma_{02}$ (ps)	$\lambda$ (cm)
$2.5 \times 2.5$	XP2020	$123 \pm 4$	$132 \pm 4$	$55 \pm 3$
$2.5 \times 2.5$	FEU-115M	$234 \pm 4$	$233 \pm 4$	$69 \pm 3$
$6.0 \times 1.25$	XP2020	$155 \pm 4$	$155 \pm 4$	$50 \pm 3$

6. When fitting data for the two  $1.25 \times 6.0$  cm<sup>2</sup> bars it was assumed that  $\lambda_1 = \lambda_2$  and that the time resolution at  $x = 0$  for the PMTs viewing the same bar are equal (see Table 1). As a result, the following parameters were derived:  $\sigma_{01} = \sigma_{02} = 159 \pm 6$  ps,  $\sigma_{03} = \sigma_{04} = 153 \pm 6$  ps and  $\lambda = 51 \pm 3$  cm. The dependence  $\sigma_2(x)$  is shown in Fig. 6.

Comparison of timing properties for the  $1.25 \times 6.0$  cm<sup>2</sup> and  $2.5 \times 6.0$  cm<sup>2</sup> bars shows that the time resolutions at the center of the bar are better by factor of  $\approx 1.4$  for the  $2.5 \times 6.0$  cm<sup>2</sup> bar (data for this bar were published in Ref. [3]). This is in agreement with relation (2). But the time resolutions at the bar edges are the same in both cases indicating that near the PMTs the time resolution does not depend on photoelectron statistics.

The time resolution of the  $1.25 \times 6.0$  cm<sup>2</sup> bar as a function of counting rate is presented in Fig. 7. It

does not depend on particle flux up to  $\approx 5 \times 10^5$  particles/s.

#### 4. Conclusions

Timing characteristics of 2 m long scintillation counters with  $1.25 \times 6.0$  and  $2.5 \times 2.5$  cm<sup>2</sup> cross-sections viewed from both ends by XP2020 and FEU-115M PMTs have been studied. The time resolution for the single  $1.25 \times 6.0$  cm<sup>2</sup> counter varies from 110 ps at the bar center to 60 ps at the ends while for the two-bar hodoscope these values are equal to 77 and 40 ps, respectively. The time resolution for the 2.5 cm square bar changes from 50(105) to 90(160) ps for the XP2020 (FEU-115M) PMT. The time resolution of the investigated counters is independent of counting rate up to  $\approx 5 \times 10^5$  particles/s.

Based on these results, the  $1.25 \times 6.0$  cm<sup>2</sup> counter equipped with the XP2020 PMTs is the optimal solution for the TOF hodoscope of the GlueX experiment. A 2.5 cm square bar viewed by FEU-115M PMTs meets the requirements of the rare kaon decay experiment.

## Acknowledgements

We appreciate financial support from the US Department of Energy, the Russian Ministry for Industry, Science and Technologies (grant 1305.2003.2) and the Russian Fund for Basic Researches (grant 02-02-17019) and valuable contributions from I. Beljakov, A. Ivashentsov, I. Shvabovich, A. Soloviev and S. Zvjagintsev.

## References

- [1] [www.gluex.org](http://www.gluex.org).
- [2] S. Denisov, et al., Nucl. Instr. and Meth. A 478 (2002) 440.
- [3] S. Denisov, et al., Nucl. Instr. and Meth. A 494 (2002) 495.
- [4] [www.apace-science.com/eljen/](http://www.apace-science.com/eljen/).
- [5] [www.bicron.com](http://www.bicron.com).
- [6] S. Belikov, et al., Preprint IHEP 96-42, Protvino, Russia, 1996 (in Russian).